Dynamic stress and strain in the bone-implant interface of total replaced hip during walking

Abstract

Background: Implant loosening is one of the most common problems occurring after total hip replacement. Important factors, such as geometrical characteristics of the implant, quality of bone tissue, implantation process, and age and lifestyle of the patient, affect the loosening. This study aims to analyze the dynamic stress and strain on the bone-implant interface in the stance phase of normal walking.

Methods: A two-dimensional model, including a femur and its artificial joint, was used for numerical simulation in ADINA software using the finite element method. Young's modulus was assumed to be 12 GPa for the bone and 210 GPa for the medical stainless steel implants. At the bone-implant interface, the coefficient of friction was assumed to be 0.22, and the model simulated the conditions of a cementless surgery. The load applied to the replaced joint head was dynamically consistent with the normal walking cycle of an individual weighing 75 kg.

Results: The results showed that the strain difference is maximal at the end stem regions of the interface. The strain difference was 1.6% at the inner edge, being 16 times that at the outer edge of the interface. The maximum stress reached about 5.7 MPa.

Conclusion: The largest strain difference occurred in the lowest area of the implant stem, which indicates the possible location of the implant loosening. This information can also be important in employing hip replacement surgery strategies and developing optimal mechanical designs of the artificial joint.

Keywords: Total hip replacement, prosthesis loosening, computer simulation, finite element analysis, gait

Received: 4 months before printing; Accepted: 10 days before printing

Mohammad N. Ashtiani*, Seyed Mohsen Mortazavi Najafabadi**

* Faculty of Medical Sciences, Tarbiat Modares University
** Faculty of Mechanical Engineering, Tarbiat Modares University

Corresponding author:
Mohammad N. Ashiani

Email Address:
mnashtiani@modares.ac.ir

Introduction

Walking is among the main daily activities involving the simultaneous activity of components of the neuro-musculoskeletal system. In the skeletal system, joints are placed between the bones to facilitate movement, as do mechanical lubricants. As energy absorbers, they also play an important role in the immediate dissipation of energy entering the body. The hip joint is a spherical joint consisting of the femur's head and the acetabular cavity. The most important complication of joint surfaces is osteoarthritis, mainly caused by excessive and intermittent compressive forces resulting from walking, running, exercise, and daily activities [1-3]. In acute cases of osteoarthritis, the contact between the femoral head and the pelvis during each loading cycle gradually destroys the cartilaginous layers of the bone and causes pain. Over recent decades, total joint replacement has been the most common treatment [4, 5], which requires a relatively complex and difficult surgery. In this surgery, the femur's upper part (head and neck) and the bone shaft's central part are removed, and the implant is placed in the femoral cavity. This surgery may involve pouring bone cement between the cavity created and the implant. In 2018, about 600,000 total hip replacement (THR) surgeries were performed in the United States and the United Kingdom, indicating the widespread use of this method [6, 7]. Obtaining patterns of mechanical stress (force divided by the contact area) distribution in a replaced hip plays an important role in the design of implants, predicting possible problems such as the need for revision or loosening of the implant..

Most studies have focused on detecting the mechanical behavior of the hip implant in the distribution of different forces, types of implants, mechanical design, or mechanical surface treatments during the manufacturing process. Some common fractures in the THR have been associated with the interface between the bone, implant, and bone cement [8-10]. Given the stress in the bone cement layers surrounded by implants, optimization-based methods have been used to reduce the stress concentration in critical areas [11, 12]. Kleeman et al. (2003) reported that changes in the hip anteversion and implant offset might cause critical conditions in the proximal femur [13]. In order to detect possible loosening of a replaced hip implant, Rowlands et al. (2008)
used an ultrasonic method, causing harmonic vibrations on the condyles of the femur and measuring the response in the greater trochanter [14]. Using finite element analysis, Kaku et al. (2020) investigated the effect of different liners on stress distribution of the acetabular cups and found that the elevated-rim liners exhibit high stress at the cup edge [15]. The possibility of a stress shielding effect in the bone tissue around the replaced hip implant and the possibility of failure in the trochanteric region are also the results of a finite element study by Abdullah et al. (2017) that simulated falling from the side [16]. Chethan et al. (2020), by performing static finite element analysis, showed that an elliptical cross-section for the hip implant stem leads to a lower stress in the bone tissue compared to the circular and trapezoidal cross-sections [17]. Another finite element study by Ismail et al. (2018) showed that the bone-implant interface could provide initial stability after surgery. This stability is the basis for achieving secondary stability and success of implantation [18].

The success of hip replacement surgery requires the primary stability of the joint. The concept of primary stability refers to the mechanical anchorage between the implant and the host bone. If all of the factors that contribute to the success of the surgery fail to provide primary stability, the possibility of secondary stability that depends on the ossification process around the implant is frustrated. Implant loosening in the THR is one of the most important indicators of the lack of primary stability in implantation. The relative displacement of the implant in the host bone tissues causes instability and micro-movement at the interface where osteoblasts are expected to form bone bridges. Therefore, the present study is aimed at investigating the effect of dynamic forces caused by normal human gait on the loosening of the replaced hip implant and its location.

Methods

This study used the finite element method to obtain mechanical stresses and strains through loading of normal gait in bones, implants, and especially their interface. This method is based on the numerical solution of mechanical-physical differential equations in an environment defined by materials and geometry, which are divided into smaller components by geometric discretization. In fact, these equations are first formed and solved for each element and then provide the structural coherence of the result throughout the environment. Hence, the first step is to define the geometry of the environment. The following steps include assigning the properties of the materials to the components present in the environment, defining the boundary conditions at the finite ends of the environment, and finally, solving the problem.

Geometrical model

A two-dimensional model of the femur (a cross-section in the frontal plane) was used in the CATIA V5 software to simulate cementless THR surgery. The head and neck of the femur, as well as a part of the bone shaft, were cut and removed in the model according to conventional orthopedic surgery (Figure 1-a). The two-dimensional design of the hip implant was placed inside the bony stem such that there was no space between the two parts of the model.

Materials

The materials used in this simulation all had linear elastic properties. The elastic modulus, Poisson's ratio, and density of the bone were equal to 12 GPa, 0.38, and 1.99 g/cm^3, respectively. The properties of the implant material were assumed equal to those of medical stainless steel with an elastic modulus of 210 GPa, Poisson's ratio of 0.30, and density of 8.62 g/cm^3 [19]. The behavior of the two materials was assumed to be completely isotropic, i.e., the properties of the materials were the same in different directions.

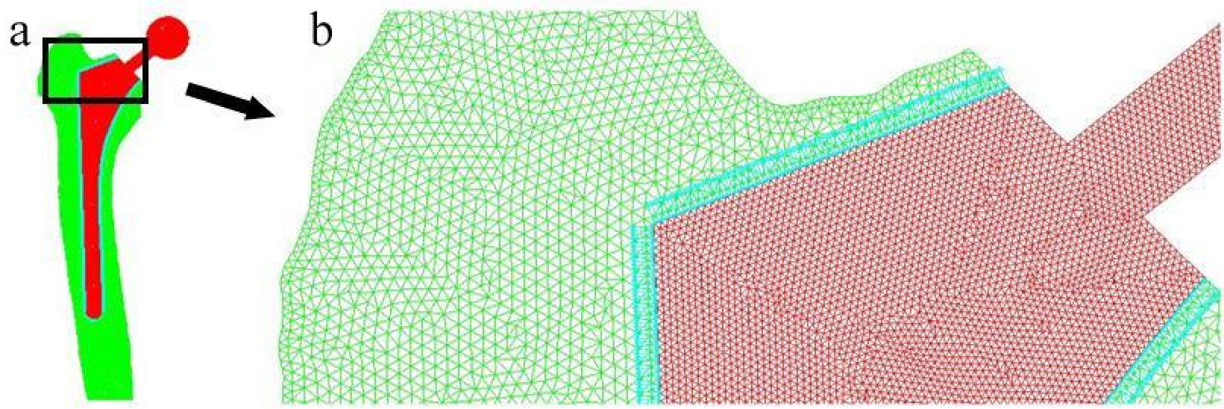

Figure 1. a) A two-dimensional model of a hip replacement implant in the femur, b) An enlarged image of finite element meshing and applying the condition of the bone-implant interface

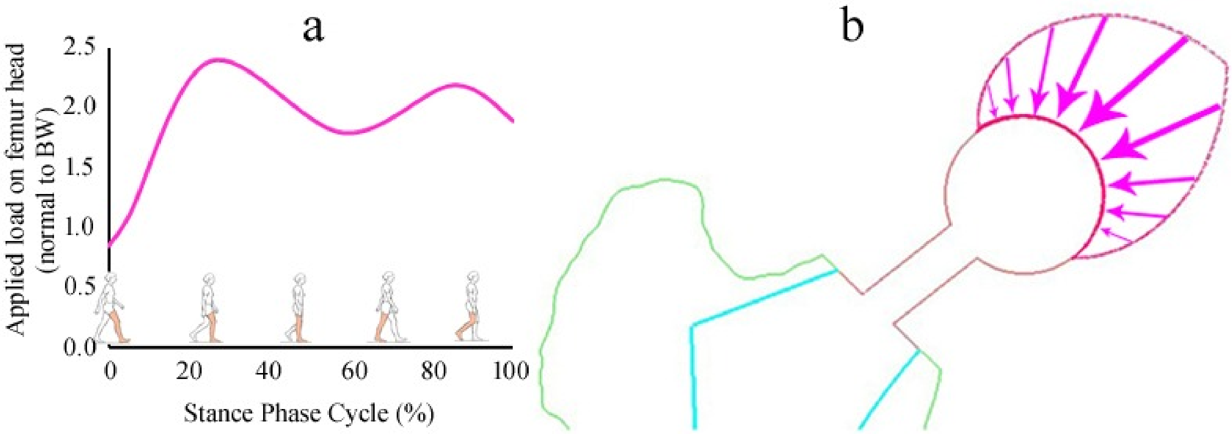

Figure 2. a) Dynamic loading in the model, b) Geometric distribution of the load on the implant head

Loading and boundary conditions

The lower surface of the model, which cuts the bone shaft in the transverse plane, was fully-restrained and had no degree of freedom of movement. In the bone-implant interface, the Coulomb coefficient of friction was assumed 0.22 to be reminiscent of the postoperative partially osseointegrated state (theoretical friction coefficient equal to infinity) [20]. Figure 1-b shows the mechanical conditions simulated in the bone-implant interface. The load was considered on the implant head according to the natural forces applied while a 75 kg-person walks [21]. The force applied to the implant head, which was transmitted from the acetabular cup, had a geometrically distributed parabolic shape as shown in Figure 2-b to be as close to reality as possible.

Numerical solution

The finite element method was used to obtain the mechanical stress distribution in the model and the strain difference at the bone-implant interface. The two-dimensional model was considered in a plane stress state (assuming that the stress perpendicular to the model plane is zero) [22]. The model consisted of 133,705 nodes and 43,641 triangular elements, of which 42% belonged to the bone and the rest to the implant. The numerical solution process was performed using the ADINA software.

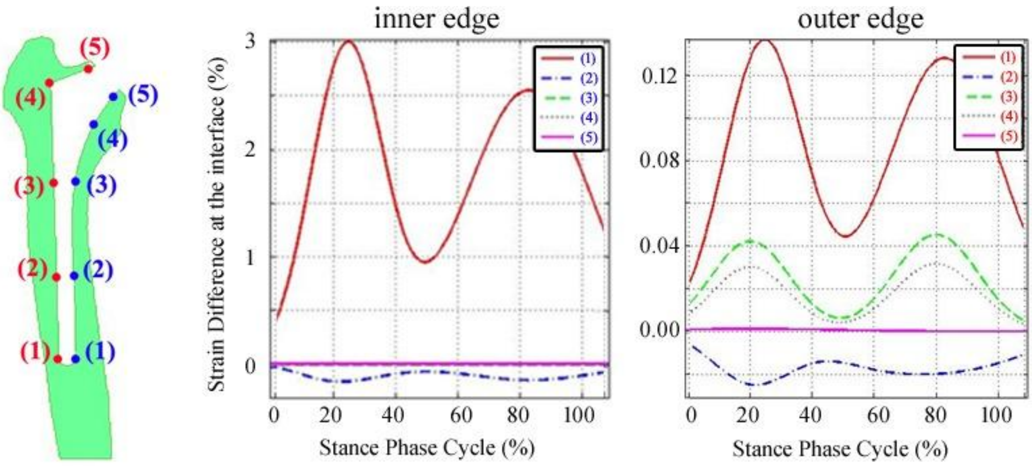

Figure 3. Marking of three points on the inner and outer edges and changes in strain difference at the joint bone-implant interface at both edges

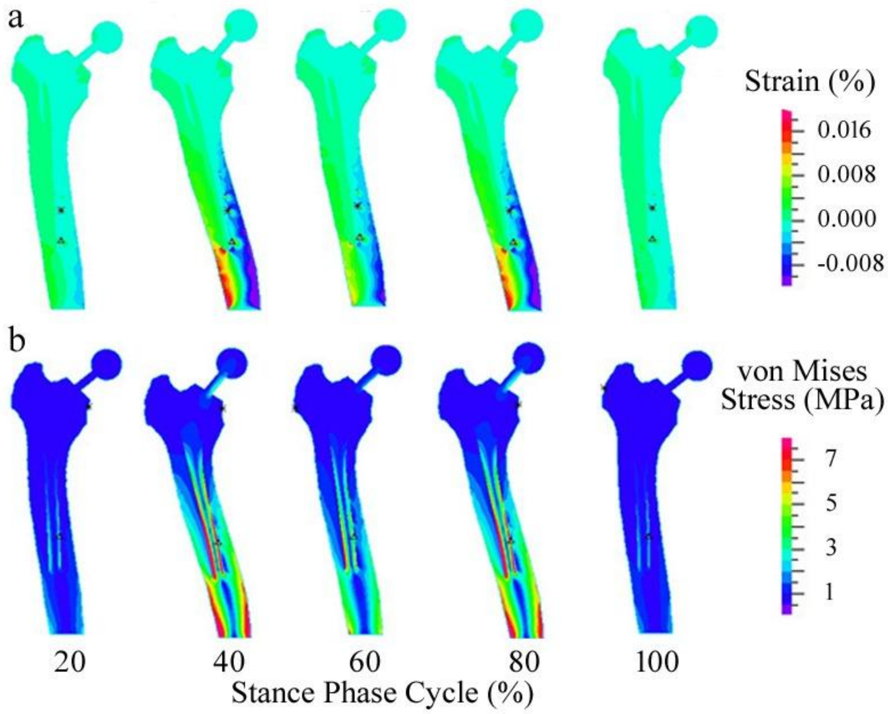

Figure 4. Contours of a) strain, b) von Mises stress in the model in different percentages of walking stance phase

Results

After numerical solution, points on the bone-implant interface were marked based on the Gruen zones' numbering system. To compare the location of sustaining mechanical stresses, three pairs of points on the bone-implant interface at both the outer and inner edges, as well as the middle of the seventh Gruen zone, were marked as shown in Figure 3. At these points, strain differences on both sides of the interface were calculated as a measure of implant looseness under load. Figure 3 depicts the time-dependent response of the horizontal component of the strain difference (i.e., along the medial-lateral direction) on both sides of the bone-implant interface. The maximum strain difference at the inner edge (with a strain of 1.6%) was about 16 times that at the outer edge (with a strain of 0.1%). The greatest interface strain difference occurred in the lowest zone of the bone-implant interface (Gruen zones 3 and 5). Moreover, the zones closer to the implant head experienced smaller strain differences. The variation of the strain difference with the percentages of the gait's stance phase was similar in all regions and was maximum at the mid-stance moment (about 25%). The second peak of strain difference changes occurred at the toe-off moment (about 85%).

Figure 4 demonstrates the mechanical strain and stress distributions in the two-dimensional section of the model. When the maximum force exerted in the walking cycle was applied to the leg at the mid-stance moment (approximately 25%), the outer part of the bone was subjected to a compressive (positive) strain, while the inner part of the bone was under tensile strain. The von Mises stress distribution, which always gives a positive quantity and is used as a measure of failure stresses, had a significant increase at the bone-implant interface compared to the surrounding environment. The lower end of the model also received significant von Mises tensions. The maximum stress in the model reached 5.7 MPa.

Discussion

In order to quantify the implant loosening in a replaced hip joint, it is possible to rely on the strain difference between the bone and the implant stem. In other words, the deformation of the hip implant with medical stainless steel compared to the deformation of the bone tissue in its vicinity can be considered a measure of separation of the two materials. If this difference increases, it means that the two adjacent materials do not necessarily deform with each other, which can lead to separation and, eventually, loosening. Figure 4-a shows this difference well on the inner edge. This diagram indicates two large peaks for strain differences at points, especially at the end of the stem (Gruen zones 3 and 5) that are repeated in each walking cycle. In the upper regions (Gruen zones 1 and 7), especially on the inner edge of the bone-implant interface, strain changes are negligible. Therefore, the risk of loosening is lower. However, in Gruen zones 3 and 5 (the end of the implant stem), the strain difference at the surface has reached a significant value of 1.6%, which may reduce the primary stability of the implantation.

The difference in strain between the bone and the implant at the outer edge shown in Figure 3 indicates that the greatest strain has occurred in the fifth Gruen zone, but the strain difference is 16 times smaller, and the maximum does not exceed 0.1%. This indicates that the risk of implant loosening at the outer edge is negligible. This finding is consistent with previous finite element studies [23, 24].

El'Sheikh et al. (2003) dynamically modeled the mechanical stresses on an artificial hip joint in a sudden fall using the finite element method [23]. Luo et al. (2020) applied a static load to a three-dimensional model before and after total hip replacement and stated that the mechanical stress in the internal and distal parts is higher in the replaced joint [24].

According to the values of the strain difference at the interface, the risk of loosening at the inner edge is higher, but as shown in Figure 4, contrasts may appear due to the greater amount of strain on the outer edge. It should be noted that the color contours shown in Figure 4 are absolute strains, while the data in Figure 3 represent the relative strains between the bone and the implant. Figure 4 also shows that the maximum deformation at the toe-off moment (before the foot leaves the ground, about 85% of the stance phase) in the walking cycle appears when the lower limb provides a propelling force. In agreement with this result and based on the mechanical stress distribution patterns in Figure 4, it can be concluded that during the initial contact until the toe-off moment, the stress is distributed only at the interface, but the amount and distribution of stress increase dramatically while bearing the load.

At about 55% of the walking cycle, when the locomotor system prepares for the swing phase, most of the leg muscles try to generate their propulsive force (in the toe-off moment). From a kinematic point of view, at this moment, the angle of the hip joint, reaching its maximum amount of extension, causes a high combined bending and torsional moment, which can change the range of mechanical stresses up to about 5.7 MPa and increase the strain differences to 1.6%. The amount of stress in normal cartilage tissue in the hip joint due to walking in the study of Li et al. (2021) was calculated to be 6.5 MPa [25]. However, it is important to note that despite using dynamic gait loading, their finite element modeling examined the natural structure of articular cartilage in the hip and did not study joint replacement [25].

Since the strain difference at the bone-implant interface is significantly high, it can be predicted based on previous sources that a high repetition rate would lead to implant failure [23]. In addition, loosening of the lower part of the implant stem at the interface with the bone adversely affects the structural integrity of the bone-implant complex, and the load-bearing share vanishes in that zone. In other words, when there is no material medium for the transfer of mechanical stress, the amount of mechanical stress is expected to increase over the other zones leading to an expanding separation.

Once the foot is in the mid-stance position (about 25% of the stance when the maximum weight is borne), the mechanical stress and strain difference at the interface rises naturally due to the bearing of the load so that the von Mises stress reaches 1.5 kPa. The strain difference at the bone-implant interface has reached 1.4%. In the initial phase of swinging, a decrease in stress and strain difference occurred at the interface, which was due to the reduction of the applied load. In addition, the values and distributions of the stress contours in Figure 4 indicate a kind of stress concentration at the bone-implant interface. The difference in the elastic moduli of the two materials (the implant is more than ten times stiffer) causes a greater share of mechanical stress flow and creates a state of stress shielding. This happens more intensely at the peaks of dynamic loading during a walking cycle, which is also noted by the previous

studies [23]. Performing a finite element study on the replaced hip joint, Todo (2018) recommended that by reducing the elastic modulus of the implant, the formation of the stress shielding and, consequently, loosening in the implant stem can be prevented to some extent [26].
The present study has some limitations. First, modeling was done with some simplifications, the most important of which were the two-dimensionality of the model and the assumption of linear elasticity and isotropy of materials (independence of material properties from geometric directions). Modeling the load on the hip prosthesis, Shaik et al. (2012) showed that the two-dimensionality of the model, assuming the plane stress state, may underestimate the results by about 14% error compared with a similar three-dimensional model in the same conditions. This error is due to the increased stiffness of the two-dimensional model (with more material in constant thickness) compared to the three-dimensional one [22]. Therefore, it is suggested to model three-dimensional geometries to analyze such cases in future studies. In addition, the friction between the bone and the implant is not actually the same throughout the interface, but it was inevitably assumed constant in this study. The boundary conditions assumed in this model were also accompanied by simplifications and the possibility of error. Cutting the bone from the diaphysis in the model and fixing all degrees of freedom differ from the actual condition in which the bone is restrained by the condyles in the knee.
Furthermore, the probability of loosening with current results is somewhat underestimated because, in reality, the load is applied cyclically and at a high frequency (at least 1 Hz) when walking, which may accelerate the reduction of primary stability. Previous studies have shown that a normal hip replacement is generally capable of withstanding one million loading cycles per year [27]. Griza et al. (2009) showed that even if the implant is proximally loosened, it can withstand up to another 5 million loading cycles [27]. However, a recent study by Babic et al. (2020) stated that the hip implant could withstand only about 350,000 loading cycles [28]. In addition, since this study assumed the implantation without bone cement, another study can investigate the effect of using cement on strain distribution and mechanical stress. The reason is that according to the theory of beam on an elastic foundation, a structure or beam (an implant stem herein) has a smaller displacement on a more elastic foundation [29].

Conclusions

The greatest strain difference occurred in the lowest zone of the implant stem, indicating the possible location of implant loosening. The inner edge of the bone-implant interface bore a greater strain difference. Unlike the outer edge, where the mechanical stress was compressive, the mechanical stress on the inner edge was tensile, which may reduce the primary stability and loosening of the implant. The results of this study suggest that the strategies aimed at preventing the loosening, either optimizing implant design or changing replacement surgery procedures, should focus on reducing tension in the internal and distal part of the implant stem (Gruen zone 5).

References

1. Ishida K. Okada K. Hamada Y. Wear and bending strain characteristics of artificial hip joint with non-glued stem and UHMWPE femur. Precis Eng. 2005;29(4):396-403. DOI:10.1016/j.precisioneng.2004.12.008.
2. Hatton A. Nevelos J. Nevelos A. Banks R. et al. Alumina–alumina artificial hip joints. Part I: a histological analysis and characterisation of wear

debris by laser capture microdissection of tissues retrieved at revision. Biomaterials. 2002;23(16):3429-40. DOI: 10.1016/s0142-9612(02)00047-9. PMID: 12099286
3. Firkins P. Tipper J. Ingham E. Stone M. et al. A novel low wearing differential hardness, ceramic-on-metal hip joint prosthesis. J Biomech. 2001;34(10):1291-8. DOI: 10.1016/s0021-9290(01)00096-3. PMID: 11522308
4. Bachir Bouiadjra BA. Belarbi A. Benbarek S. et al. FE analysis of the behaviour of microcracks in the cement mantle of reconstructed acetabulum in the total hip prosthesis. Computat Mater Sci. 2007;40(4):485-91. DOI:10.1016/j.commatsci.2007.02.006
5. Lannocca M. Varini E. Cappello A. et al. Intra-operative evaluation of cementless hip implant stability: A prototype device based on vibration analysis. Med Eng physics. 2007;29(8):886-94.
6. 6. Kremers HM, Larson DR, Crowson CS, et al. Prevalence of total hip and knee replacement in the United States. J Bone Joint Surg (Am Vol). 2015;97(17):1386-97.
7. Culliford DJ, Maskell J, Beard DJ, Murray DW, Price AJ, Arden NK. Temporal trends in hip and knee replacement in the United Kingdom: 1991 to 2006. J Bone Joint Surg (Br Vol). 2010;92(1):130-5.
8. Beckenbaugh RD. Ilstrup DM. Total hip arthroplasty. J Bone Joint Surg Am. 1978;60(3):306-13. PMID: 649633
9. Maloney WJ. Schmalzried T. Harris WH. Analysis of long-term cemented total hip arthroplasty retrievals. Clin Orthop Relat Res. 2002;405:70-8. DOI: 10.1097/00003086-200212000-00009. PMID: 12461358
10. Jasty M. Maloney W. Bragdon C. O'connor D. et al. The initiation of failure in cemented femoral components of hip arthroplasties. J Bone Joint Surg Br. 1991;73(4):551-8. DOI: 10.1302/0301-620X.73B4.2071634. PMID: 2071634
11. Huiskes R. Boeklagen R. Mathematical shape optimization of hip prosthesis design. J Biomech. 1989;22(8-9):793-804. DOI: 10.1016/0021-9290(89)90063-8. PMID: 2613715
12. Katoozian H. Davy DT. Effects of loading conditions and objective function on three-dimensional shape optimization of femoral components of hip endoprostheses. Med Eng Phys. 2000;22(4):243-51. DOI: 10.1016/s1350-4533(00)00030-8. PMID: 11018456
13. Kleemann RU. Heller MO. Stoeckle U. et al. THA loading arising from increased femoral anteversion and offset may lead to critical cement stresses. J Orthop Res. 2003;21(5):767-74. DOI: 10.1016/S0736-0266(03)00040-8. PMID: 12919861
14. Rowlands A. Duck F. Cunningham J. Bone vibration measurement using ultrasound: Application to detection of hip prosthesis loosening. Med Eng Physics. 2008;30(3):278-84.
15. Kaku N, Tanaka A, Tagomori H, Tsumura H. Finite element analysis of stress distribution in flat and elevated-rim polyethylene acetabular liners. Clin Orthop Surg. 2020;12(3):291-7.
16. Abdullah AH. Todo M. Nakashima Y. Stress and damage formation analysis in hip arthroplasties using CT-based finite element method. J Eng Appl Sci. 2017;12(10):2715-9. DOI:10.3923/jeasci.2017.2715.2719
17. Chethan KN. Zuber M. Bhat SN. Et al. Static structural analysis of different stem designs used in total hip arthroplasty using finite element method. Heliyon. 2019;5(6):e01767. DOI:10.1016/j.heliyon.2019.e01767. PMID: 31245635 PMCID: PMC6581841
18. Ismail NF. Shuib S. Yahaya MA. Et al. Finite element analysis of uncemented total hip replacement: The effect of bone-implant interface. Int J Eng Technol. (UAE). 2018;7(4):230-4.
19. Stolk J. Verdonschot N. Cristofolini L. et al. Finite element and experimental models of cemented hip joint reconstructions can produce similar bone and cement strains in pre-clinical tests. J Biomech. 2002;35(4):499-510. DOI: 10.1016/s0021-9290(01)00213-5. PMID: 11934419
20. Peter B. Ramaniraka N. Rakotomanana L. et al. Peri-implant bone remodeling after total hip replacement combined with systemic alendronate treatment: a finite element analysis. Computer Method Biomech Biomed Eng. 2004;7(2):73-8.
21. Kennedy F. Biomechanics of the hip and knee: implant wear. Wear of orthopaedic implants and artificial joints: Elsevier; 2013. p. 56-92.
22. Shaik S. Bose K. Cherukuri H. A study of durability of hip implants. Mater Design. 2012;42:230-7.
23. El'Sheikh H. MacDonald BJ. Hashmi MSJ. Finite element simulation of the hip joint during stumbling: a comparison between static and dynamic loading. J Mater Process Technol. 2003;143:249-55.
24. Luo C. Wu XD. Wan Y. Liao J. et al. Femoral Stress Changes after Total Hip Arthroplasty with the Ribbed Prosthesis: A Finite Element Analysis. BioMed Res Int. 2020; 2020(40):1-8. DOI:10.1155/2020/6783936
25. Li J. Development and validation of a finite-element musculoskeletal model incorporating a deformable contact model of the hip joint during gait. J Mechan Behav Biomed Mater. 2021;113:104136.

26. Todo M. Biomechanical analysis of hip joint arthroplasties using CT-image based finite element method. J Surgery Res. 2018;1(2):34-41.
27. Griza S. Zanon G. Silva E. Bertoni F. et al. Design aspects involved in a cemented THA stem failure case. Eng Failure Anal. 2009;16(1):512-20. DOI:10.1016/j.engfailanal.2008.06.016
28. Babić M. Verić O. Božić Ž. Sušić A. Finite element modelling and fatigue life assessment of a cemented total hip prosthesis based on 3D scanning. Eng Failure Anal. 2020;113:104536.
29. Boresi AP. Schmidt RJ. Sidebottom OM. Advanced mechanics of materials: Wiley New York; 1985.